Bachiller Martin, MC.; Esteban González, H.; Morro Ros, JV.; Boria Esbert, VE. (2011). Hybrid mode matching method for the efficient analysis of rods in waveguide structures. Mathematical and Computer Modelling. 57(7-8):1832-1839. doi:10.1016/j.mcm.2011.11.076.

Hybrid mode matching method for the efficient analysis of rods in waveguided structures

C. Bachiller, H. Esteban, J.V. Morro, V. Boria,

Departamento de Comunicaciones
Universidad Politécnica de Valencia
Camino de Vera S/N, 46022 Valencia, Spain

Abstract

Traditionally metallic waveguide filters have been used commercially for microwave applications. These filters have very reduced insertion losses within their operating frequency band and their construction is considerably economic. On the other hand, metallic filters have significant drawbacks, especially when they are designed for satellite and other spatial applications, since their weight and size may very often be too high and due to the lack of atmosphere, the Multipactor effect limits considerably the power that the filters can handle . This problems can be reduced by using new topologies of H-plane waveguide filters loaded with dielectric resonators. Nevertheless the analysis and design of these filters is far more complex than the one of all metallic filters, due to their special topology. Efficient mathematical tools are required for this analysis and this paper presents a new hybrid mode matching method for the efficient analysis of rods in waveguided structures.

Key words: Communications, microwave filters, rectangular waveguides, dielectric loaded waveguides, applications of the fast Fourier Transform, Bessel and Hankel functions, Mode Matching methods

1 Introduction

Filtering is one of the main processes in any communication system. The signals arriving to the receptor must be filtered in frequency before being demoduled and processed. The different frequencies and applications define the

Email address: mabacmar@dcom.upv.es (C. Bachiller, H. Esteban, J.V. Morro, V. Boria).

technology used to manufacture the filters. For space communication applications the traditional filters are built with waveguided structures [10], as shown in Figure 9(a). The structure is divided into cavities separated by obstacles (posts, irises, etc.) which resonate at the central frequency of the filter. The number of cavities defines the order of the filter and the size and position of the obstacles determine its bandwidth.

There are many reasons that lead to develop new topologies of high frequency filters for space applications. The traditional all metal waveguide resonant cavities are heavy and bulky, in many cases they are a limiting factor in the payload of a satellite. When including dielectric rods inside the resonant cavities, the size of the whole structure is dramatically reduced. Ceramic dielectrics with high dielectric constant and temperature stability are commercially available. They allow to implement small size, good temperature stability, and high-Q dielectric resonators [1]. If the height of the dielectric posts is the same as the height of the waveguide, that is, if the posts are all inductive or H-plane, better out of band rejection and Multipactor response can be obtained [3].

Different topologies of this new generation of filters can be implemented as shown in Figure 1.

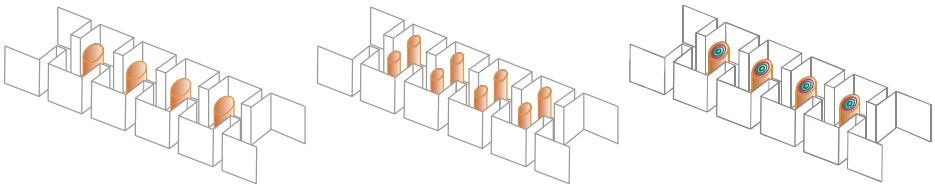

(a) Centered. (b) Double. (c) Multilayered.

Figure 1. Cavities filters with dielectric resonators.

Another step in the design of high performance filters are evanescent filters in H-plane, see Figure 2. They are even smaller than the cavities filters and present the widest out of band rejection [6,7].

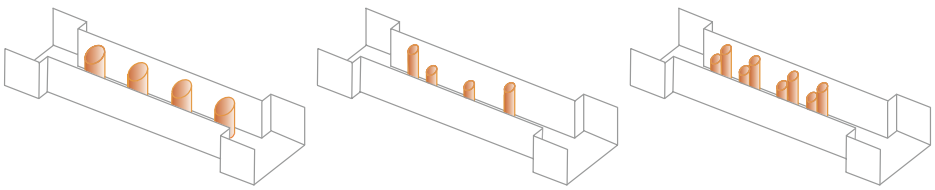

(a) Centered. (b) Off-centered. (c) Double.

Figure 2. Evanescent H-plane filters with dielectric resonators.

Nevertheless the accurate modeling of the circular dielectric resonators is far more complex than the analysis of square metal structures, since circular and rectangular geometries must be analyzed together. The authors have developed a technique for the analysis of these passive devices which consists of dividing the device into simpler building blocks: empty waveguides, steps and

sections of waveguide loaded with the dielectric or metallic posts, as shown in Figure 3. The elements of the generalized scattering matrix are the parameters that characterize the frequency response of the structure. The matrix of each block is obtained by the most suitable analysis method, and then all the matrices are connected by a new and efficient iterative technique that provides the generalized scattering matrix of the whole filter [2].

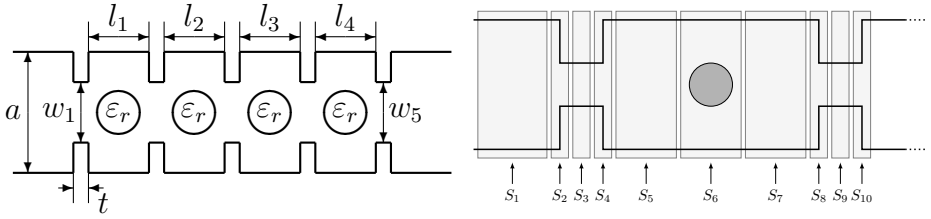

(a) Filter (b) Segmentation

Figure 3. Analysis strategy

The generalized scattering matrix of the empty sections of the waveguide is well known from the literature, and the waveguide steps can be analyzed by means of several modal techniques, such as the well know mode matching method [11] or the integral equation technique [8].

However, the analysis of waveguide sections loaded with circular obstacles is far more complex. In order to characterize these structures, circular and rectangular geometries must be considered at the same time. This complexity in the geometry makes it difficult to use purely analytic techniques, while the numerical methods are highly time-consuming. This is a serious drawback when using the simulator in a design process, since it typically demands a huge number of simulations before it finds a suitable design that fulfills the specifications. For this reason the accurate and efficient analysis of H-plane circular rods inside rectangular waveguides has received considerable attention for more than 60 years.

In this paper the authors propose a method for this analysis of the structure by decomposing the electromagnetic fields in two different regions: near the cylindrical post as cylindrical modes and far away as guided modes . The cylindrical field waves are series expansions of Bessel and Hankel functions and the field guided waves are series expansions of sinusoid functions [9]. Then a circular boundary is used to match cylindrical and guided waves. The method increases the accuracy and stability of the analysis, no matter the number of modes or the nature of the H-plane problem under study. This is accomplished with a new mode matching procedure which uses the fast Fourier transform to solve the matching between cylindrical and guided modes [4]. The method described in [9] has the limitation that the access ports of the structures need a certain distance so that the method successfully converges to the solution. This does not happen in the case of filters with dielectric resonators, where the access ports are too close to the resonators. The authors propose to make the

modal coupling between modes of open space and guided along a circle that touches the walls of the guide. It is necessary to solve the coupling differently than is done in [9], projecting on both internal and external modes to the circumference, unlike in [9] where only projected on external modes (guided). Analytical expressions are used to characterize the circular posts in the inner region, thus resulting in a highly efficient technique for the analysis of single or multiple posts inside a rectangular waveguide.

The results of the work were assessed by the automated design of a filter with dielectric rods by a CAD tool, the manufacture of a prototype and the measurement of its frequency response.

2 Efficient Analysis of the Filters

The method used for the efficient analysis of the waveguide segments with multiple circular dielectric rods is the one described in [4]. In order to characterize one o various dielectric rods placed inside a rectangular waveguide, two regions are defined (see Fig. 4).

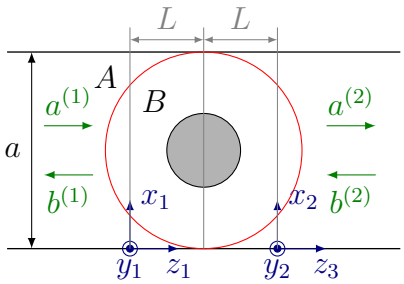

Figure 4. General layout of the problem and different regions for the analysis method

In region B the field is expanded as summations of incident and scattered cylindrical open space modes,

$$\overrightarrow{E} = \overrightarrow{E}^{in}(\rho,\phi) + \overrightarrow{E}^{sc}(\rho,\phi) \tag{1}$$

$$\overrightarrow{E}^{in}(\rho,\phi) = \sum_{n=-N_i}^{N_i} i_n J_n(k\rho) e^{jn\phi}\hat{z} \tag{2}$$

$$\overrightarrow{E}^{sc}(\rho,\phi) = \sum_{q=-N_{sc}}^{N_{sc}} c_q H_q^{(2)}(k\rho) e^{jq\phi}\hat{z} \tag{3}$$

where i_n and c_q are the incident and scattered field spectra in open space, $J_n(k\rho(\phi))e^{jn\phi}$ and $H_q^{(2)}(k\rho(\phi))e^{jq\phi}$ are the n-th incident and q-th scattered cylindrical modes, and N_i and N_{sc} are the truncation indexes for the summa-

tions of incident and scattered cylindrical modes. Both numbers must be high enough to ensure good accuracy of the results [9].

In the outer region, or region A, the tangential fields are expanded as summations of the guided modes of the canonical rectangular waveguide. Since both the geometry and the excitation are invariant in height (dimension y), only the family of TE_{m0} modes are considered, and the fields can be expanded as

$$\vec{E}_t^{(i)} = \sum_{m=1}^{Mi} (a_m^{(i)} e^{-\gamma_m^{(i)} z_i} + b_m^{(i)} e^{\gamma_m^{(i)} z_i}) \vec{e}_m^{(i)'}(x_i) \tag{4}$$

$$\vec{H}_t^{(i)} = \sum_{m=1}^{Mi} (a_m^{(i)} e^{-\gamma_m^{(i)} z_i} - b_m^{(i)} e^{\gamma_m^{(i)} z_i}) Y_{0m}^{(i)} \vec{h}_m^{(i)'}(x_i) \tag{5}$$

where $i = 1$ for the input port and $i = 2$ for the output port, and

$$\vec{e}_m^{(i)'}(x_i) = \hat{y}_i \sqrt{\frac{2Z_{0m}^{(i)}}{a_i b_i}} \sin\left(\frac{m\pi}{a_i} x_i\right) \tag{6}$$

$$\vec{h}_m^{(i)'}(x_i) = -\hat{x}_i \sqrt{\frac{2Z_{0m}^{(i)}}{a_i b_i}} \sin\left(\frac{m\pi}{a_i} x_i\right) \tag{7}$$

$$\gamma_m^{(i)} = \sqrt{\left(\frac{m\pi}{a_i}\right)^2 - k^2} \tag{8}$$

$$Y_{0m}^{(i)} = \frac{1}{Z_{0m}^{(i)}} = \frac{\gamma_m^{(i)}}{jw\mu} = \frac{\gamma_m^{(i)}}{jk\eta} \tag{9}$$

In these equations

- m is the index of the correspondent guided mode.
- M_i, a_i and b_i are, respectively, the number of guided modes, the width and the height of the input ($i = 1$) and output ($i = 2$) ports. In the structures considered in this work $M_2 = M_1$, $a_2 = a_1$ and $b_2 = b_1$.
- $a_m^{(i)}$ and $b_m^{(i)}$ are, respectively, the amplitudes of the waves in the input ($i = 1$) and output ($i = 2$) ports.
- x_i and z_i are the coordinates local to the input ($i = 1$) and output ($i = 2$) waveguides (see Fig. 4).

Next a mode matching is performed between the guided modes of region A and the cylindrical modes of region B, enforcing the continuity of the tangential electric and magnetic fields across the circular boundary and projecting the resulting equations to the modes of regions A and B.

This process (see [4]) finally leads to the following expression for the general-

ized scattering matrix of the multiple dielectric rods inside the waveguide,

$$S = (T + RI^{-1}K)^{-1}(U - RI^{-1}J) \tag{10}$$

Where

$$T_{mn} = \int_0^{2\pi} e_n^-(\phi) g_n(\phi) Y_{0n} g_m^*(\phi) d\phi \tag{11}$$

$$R_{mn} = \int_0^{2\pi} (B_n \sin(\phi) + C_n \cos(\phi)) e^{jn\phi} g_m^*(\phi) d\phi \tag{12}$$

$$A_n = [J_n(KR) + d_n H_n^{(2)}(KR)] \tag{13}$$

$$B_n = -\frac{1}{\eta}\frac{n}{KR} A_n \tag{14}$$

$$C_n = -\frac{1}{\eta}(J_n'(KR) + d_n \cdot H_n^{(2)'}(KR)) \tag{15}$$

$$K_{mn} = \int_0^{2\pi} e_n^-(\phi) g_n(\phi) e^{-jm\phi} d\phi \tag{16}$$

$$J_{mn} = \int_0^{2\pi} e_n^+(\phi) g_n(\phi) e^{-jm\phi} d\phi \tag{17}$$

$$U_{mn} = \int_0^{2\pi} e_n^+(\phi) g_n(\phi) Y_{0n} g_m^*(\phi) d\phi \tag{18}$$

The integrals needed to fill matrices I, J, K, R, T and U can be solved either analytically or by using the fast Fourier transform.

3 Results and Conclusions

In this section a traditional all metallic filter and a filter with centered circular dielectric rods have been design to present the same electrical response. Then both filters have been manufactured and measured.

The filters were designed to have a Chebychev response in the X-band (centered at 11 GHz) with a bandwidth of 300 MHz and return losses greater than 20 dB, as shown in Figure 5.

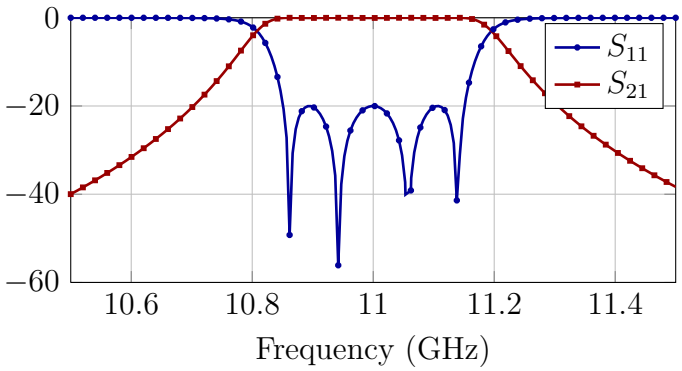

Figure 5. Ideal response for an X-band Chebychev filter. Bandwidth 300 MHz, return losses over 20 dB.

3.1 Metal Resonant Cavities Filter.

A 3-D view of the metallic resonant filter is shown in perspective in Figure 9(a). Figure 6 shows the top view, the and design parameters are listed in Table 3.1. This is a classical filter, which has been designed and analyzed in the literature on multiple occasions [5]. In this case, this classical filter was designed and analyzed in order to allow equal comparison with the new filter with dielectric rods also studied in this work.

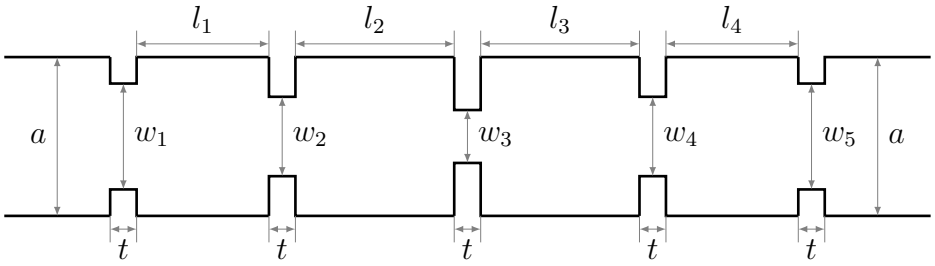

Figure 6. All metallic filter.

The filter was fabricated by the company Pinach S.L. (Alborache, Valencia, Spain) using a precision milling system and electroforming in the inner corners of the cavities. This system provides a nominal accuracy of 30 microns. The fabricated filter is shown in Figure 9(a). A dimensional control of the filter was commissioned to AIMME Metalworking Technology Institute. This dimensional control showed that there was a systematic drift so that all the dimensions of the manufactured filter were around 80 microns smaller than the nominal average value.

Finally, Figure 7 depicts the measured frequency response of the manufactured filter together with the simulated response of the designed filter. It can be observed that in the measured response there is an increase of the losses, due mainly to losses in the connectors used to perform the measurements, a

Metal Cavities Filter	
a	19,05 mm
b (height)	9,525 mm
t	2 mm
w_1, w_5	10,52 mm
w_2, w_4	7,098 mm
w_3	6,52 mm
l_0, l_5 (input and output lines)	10 mm
l_1, l_4	15,68 mm
l_2, l_3	17,605 mm
Overall length without input and output lines	76,57 mm
Overall length	96,57 mm

Table 1
Design parameters.

frequency shift of about 40 MHz and a decrease in the bandwidth. This is due to the fact that the real dimensions of the resonant cavities are around 80 microns smaller than the nominal values. This makes that the central frequency increases in frequency and the bandwidth decreases slightly. The simulated response of the same filter but corrected with the dimensions provided by the dimensional control is also shown in Figure 7. It can be observed that the response of the measurements and the simulated response of the corrected filter are in good agreement, thus proving that the analysis method provides very accurate results.

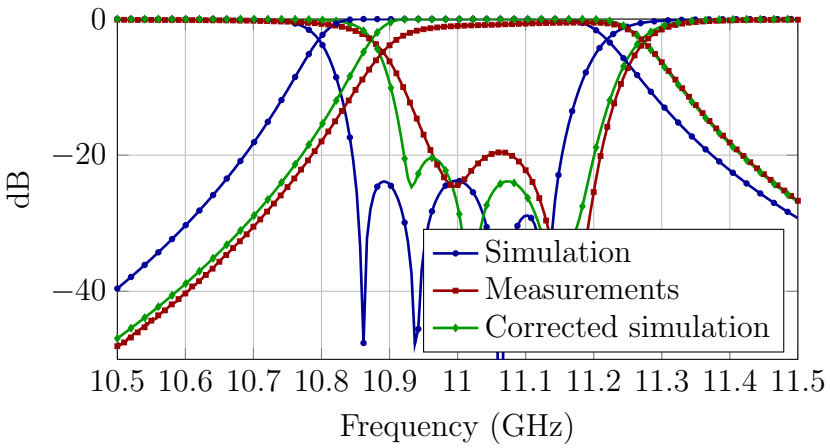

Figure 7. Results for the all metallic filter.

3.2 Cavities Filter with Dielectric Resonators

In this section the analysis technique here presented is used to design the same band-pass filter of the previous section as specified in Figure 5. But this time the topology of the filter is an H plane filter with coupled cavities and circular dielectric posts placed in the center of each cavity. The 3-D view of the filter is shown in Figure 1, and the top view in Figure 8. Table 2 contains the dimensions of the designed filter.

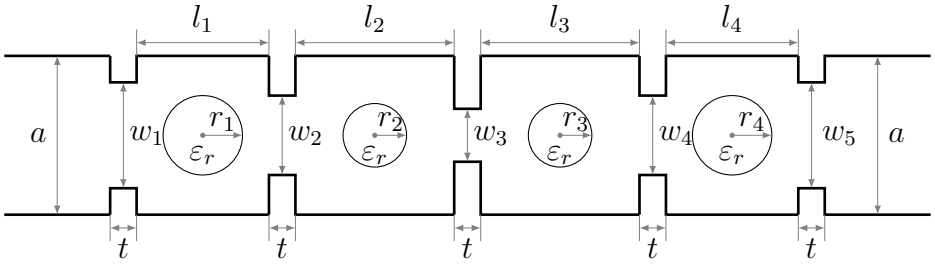

Figure 8. Filter with dielectric resonators.

Cavities Filter with Dielectric Resonators	
a	19,05 mm
b (height)	9,525 mm
t	2 mm
w_1, w_5	10,37 mm
w_2, w_4	6,286 mm
w_3	6,1 mm
l_0, l_5 (input and output lines)	10 mm
l_1, l_4	6,98 mm
l_2, l_3	8,28 mm
r_1, r_4	2,111 mm
r_2, r_3	2,172 mm
ϵ_r	24
Overall length without input and output lines	40,52 mm
Overall length	60,52 mm

Table 2
Design parameters of the filter with dielectric resonators.

This new filter was also manufactured by Pinach S.L. Once the metal structure was made the dielectric cylinders were fixed to it using an epoxy resin. The manufactured filter is shown in Figure 9(b).

A dimensional control was also commissioned to AIMME Metalworking Technology Institute for the filter with dielectric rods. This time the dimensional

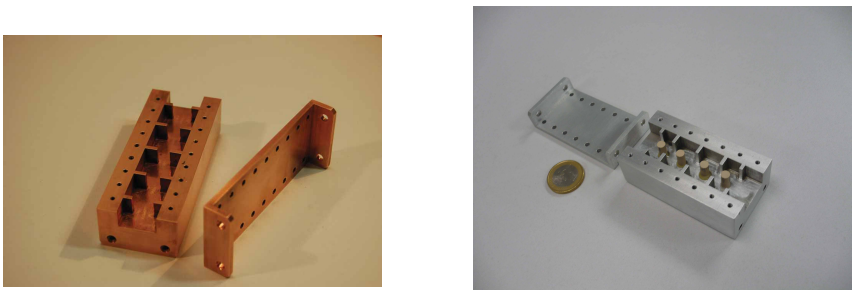

(a) All metal. (b) With dielectrics.

Figure 9. Manufactured filters.

control showed that there was again a systematic drift of around 80 microns in the inner dimensions of the metal structure, and it also showed that the diameters of the cylinders had maximum variations of ±20 microns, but the drift was random.

When the measured and simulated results were compared, there was no agreement, even if the simulation was made with the proper dimensions provided by the dimensional control. So the permittivity of the cylinders was accurately calculated, since the manufacturer stated that the tolerances for the permittivity and loss tangent were wide and they varied with the frequency. In order to measure the permittivity and loss tangent of the dielectric rods, a section of WR90 waveguide with a small recess to place a dielectric cylinder was built. In this structure the dielectric cylinder was placed in the center, see Figure 10(a), and the frequency response of the structure was measured. Then the analysis tool was used to calculate the frequency response of the structure and an optimization algorithm, the Nelder-Mead simplex method [12], was used to iteratively change the values of permittivity and loss tangent in the simulations until the simulated response was in good agreement with the measured response, as shown in Figure 10(b). This agreement between measurement and simulations was obtained with a permittivity of 18.85 and a loss tangent of 0.002.

Once the permittivity is fixed to 18.85 and the loss tangent to 0.002, a new simulation is performed and compared to the measurements in Figure 11. It can be observed that there is good agreement in both responses in the central frequency and in the bandwidth. The difference in the return losses may be due to additional losses introduced by the connectors.

3.3 Conclusions

It is possible the efficient analysis of a complex waveguide structure if it is segmented adequately. In this work a waveguide topology of H-plane waveg-

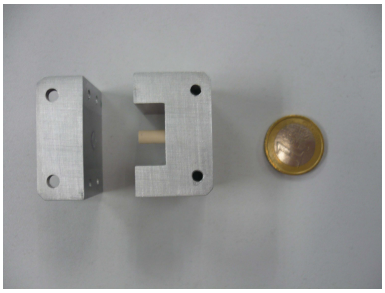

(a) Measurement setup

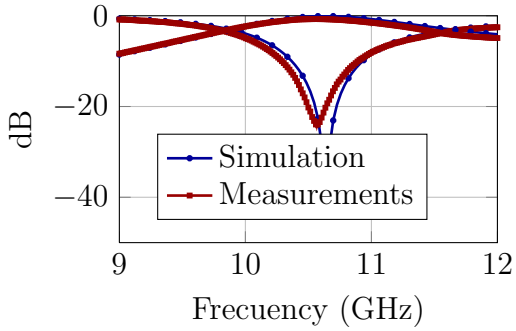

(b) Measured and simulated ($\varepsilon_r = 18.85$, $\tan\delta = 0,002$) reflexion and transmission parameters

Figure 10. Estimation of the permittivity and loss tangent of the dielectric cylinders.

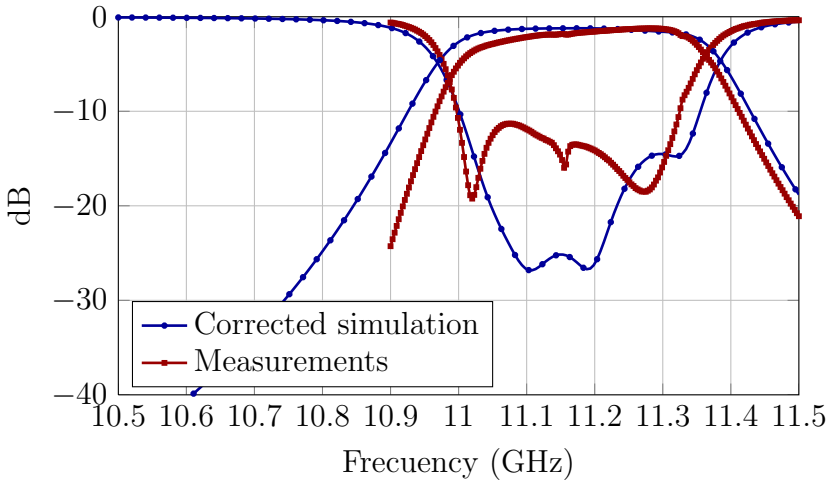

Figure 11. Reflexion and transmission of the filter simulated with $\epsilon_r = 18,85$, $\tan\delta = 2 \cdot 10^{-3}$, compared to the measurements.

uide filters with dielectric cylinders, whose analysis and design is complex, but that has advantages over traditional topologies, has been successfully designed, manufactured and measured. For the analysis of these filters a hybrid technique developed by the authors has been used. This technique expands the field near the cylinders using open space modes (Bessel and Hankel functions), and guided modes in the accessing ports. Then a mode matching is performed between open space and guided modes and the generalized scattering matrix is obtained. All the integral needed to solve the problem can be efficiently computed using the fast Fourier transform thanks to the use of a circular boundary between open space and guided modes.

References

[1] P. Arcioni, V. E. Boria, M. Bozzi, G. Conciauro, and B. Gimeno. Analysis of H-plane waveguide components with dielectric obstacles by the BI-RME method. In *Proc. of the 32nd Eu. Microwave Conf.*, pages 1–3, Milano, 2002.

[2] C. Bachiller, H. Esteban, V. E. Boria, A. Belenguer, and J. V. Morro. Efficient technique for the cascade connection of multiple two port scattering matrices. *IEEE Transactions on Microwave Theory and Techniques*, 55(9):1880–1886, September 2007.

[3] C. Bachiller, H. Esteban, F. Diaz, V.E. Boria, and J.V. Morro. Comparative study of multipactor breakdown in waveguide H-plane filters loaded with dielectric resonators. In *Int. Workshop on Multipactor, Corona and Passive Intermodulation*, pages 1–8, Valencia, Sept. 2008.

[4] C. Bachiller, H. Esteban, H. Mata, M.A. Valdes, V.E. Boria, A. Belenguer, and J.V. Morro. Hybrid mode matching method for the efficient analysis of metal and dielectric rods in h plane rectangular waveguide devices. *Microwave Theory and Techniques, IEEE Transactions on*, 58(12):3634 –3644, dec. 2010.

[5] V. E. Boria. *Análisis de problemas electromagnéticos mediante métodos modales y matrices generalizadas, y aplicaciones.* PhD thesis, Universidad Politécnica de Valencia, Valencia, 1997.

[6] V.E. Boria, M. Bozzi, D. Camilleri, A. Coves, H. Esteban, B. Gimeno, M. Guglielmi, and L. Polini. Contributions to the analysis and design of all-inductive filters with dielectric resonators. In *Proc. of EUMW 2003 European Microwave Week*, pages 1247–1250, Munich, Oct. 2003.

[7] M. Capurso, M. Piloni, and M. Guglielmi. Resonant aperture filters: Improved out-of-band rejection and size reduction. In *Proc. of the 31st Eu. Microwave Conf.*, pages 331–334, London, 2001.

[8] G. Conciauro, M. Bressan, and C. Zuffada. Waveguide modes via an integral equation leading to a linear matrix eigenvalue problem. *IEEE Trans. Microwave Theory Tech.*, 32(11):1495–1504, Nov. 1984.

[9] H. Esteban, S. Cogollos, V. E. Boria, A. San Blas, and M. Ferrando. A new hybrid mode-matching/numerical method for the analysis of arbitrarily shaped inductive obstacles and discontinuities in rectangular waveguides. *IEEE Trans. Microwave Theory Tech.*, 50(4):1219–1224, April 2002.

[10] M. Bousquet G. Maral. *Satellite Communications Systems. Systems, Techniques and Technologies.* John Wiley & Sons Inc., Chichester, 1998.

[11] R.F. Harrington. *Field Computation by Moment Methods.* The Mac Millan Company, New York, 1968.

[12] J.A. Nelder and R. Mead. A simplex method for function minimization. *Computer J.*, 7:308–313, Jan. 1965.